Supplementary material for LHCb-PAPER-2015-056

Correlation between o_2 and $\bar{o}_2$

To interpret the NN2 output as a mistag probability, a new variable, o_2, is defined in Eq. 4, which has a mirrored distribution for initial B_s^0 and $\overline{B}_s^0$ mesons of the same kinematics. For convenience, Eq. 4 is reported here again,

$$o_2' = \frac{o_2 + (1 - \bar{o}_2)}{2}, \tag{1}$$

where $\bar{o}_2$ stands for the NN2 output with the charged-conjugated input variables, *i.e.* for a specific candidate, $\bar{o}_2$ is evaluated by flipping the charge signs of the input variables of NN2. In Fig. 1, the correlation between o_2 and $\bar{o}_2$ is shown using the simulated events described in Sect. 3.

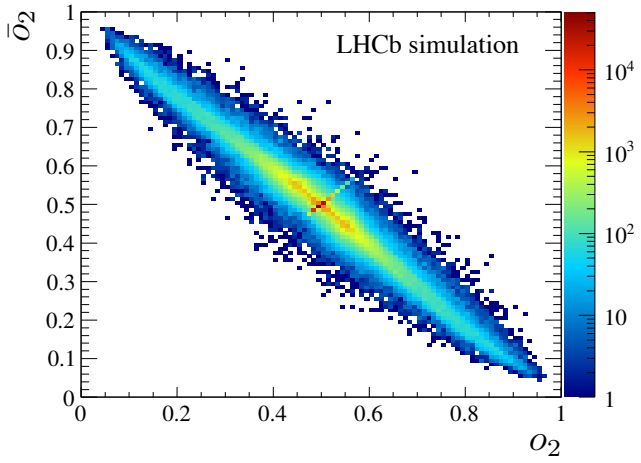

Figure 1: Distribution of $\bar{o}_2$ versus o_2 of simulated $B_s^0 \to D_s^- \pi^+$ events.

Mixing asymmetry

To illustrate the ability to resolve the fast mixing frequency in the $B_s^0 \to D_s^- \pi^+$ mode, which is a prerequisite to performing the tagging calibration, the time-dependent asymmetry is shown in Fig. 2. It is defined as

$$\mathcal{A}(t) = \frac{N_{\text{unmixed}}(t) - N_{\text{mixed}}(t)}{N_{\text{unmixed}}(t) + N_{\text{mixed}}(t)}, \tag{2}$$

where N_{unmixed} and N_{mixed} are the numbers of candidates which are tagged to have the same or a different flavour at production and decay, respectively. The horizontal axis shows the decay time modulo $2\pi/\Delta m_s$. The offset $t_0 = 0.2\,\text{ps}$ corresponds to the preselection

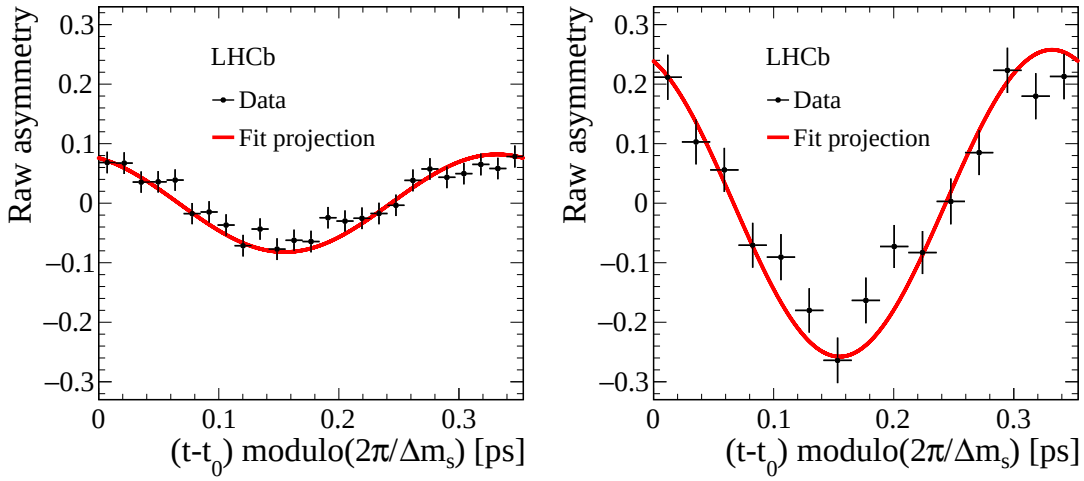

Figure 2: Time-dependent asymmetry of $B_s^0 \to D_s^- \pi^+$ signal candidates tagged as mixed or unmixed events for (left) all B_s^0 candidates and (right) candidates with a calibrated mistag probability smaller than 0.35.

requirement on the B_s^0 meson decay time. The plot in Fig. 2(left) contains all B_s^0 signal candidates, while for the plot in Fig. 2(right) only candidates with a calibrated mistag probability smaller than 0.35 are used. These plots serve for illustration only; they are not used to develop the algorithm, since they contain less information than the actual calibration procedure.

Portability check in simulation

To cross-check the portability of the calibration between different modes, we have calibrated the SSK on $B_s^0 \to J/\psi\,\phi$, $B_s^0 \to D_s^- \pi^+$ and $B_s^0 \to D_s^+ D_s^-$ candidates in simulated data. In Fig. 3 and in Table 1 the calibrations obtained with these three samples are reported. The calibration parameters are obtained exploiting the information on the true initial flavour available in simulation. The value of $p_0 - \langle\eta\rangle$ is compatible with zero in the three cases and the curves are in agreement, although there is a small deviation in the p_1 value of the $B_s^0 \to D_s^+ D_s^-$ decay with respect to the other decays. Such a deviation is understood as being related to differences in the phase space. In fact it is strongly reduced if the samples are re-weighted to match the $B_s^0 \to D_s^+ D_s^-$ transverse momentum distribution (Fig. 3(right), Table 1). These differences are covered by the systematic uncertainties on the calibration parameters given in the paper.

A similar check is done applying the calibration derived from simulated $B_s^0 \to D_s^- \pi^+$ data to simulated $B_{s2}^*(5840)^0$ candidates. The $B_{s2}^*(5840)^0$ transverse momentum distribution is weighted to match that of the $B_s^0 \to D_s^- \pi^+$ candidates. The result is displayed in Fig. 4. The calibration parameters p_1 and $p_0 - \langle\eta\rangle$ derived from the weighted $B_{s2}^*(5840)^0$

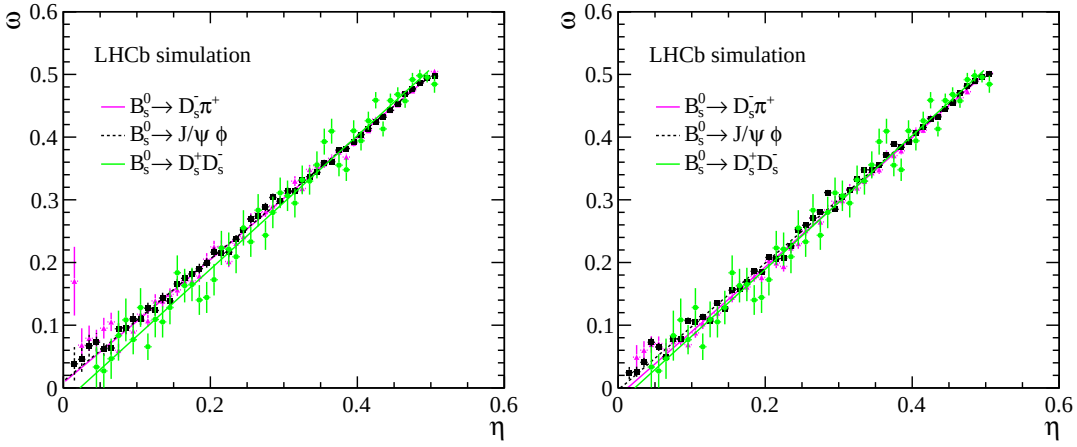

Figure 3: Calibration plots of the SSK tagging algorithm in different Monte Carlo samples. On the left, the result of the calibration without weighting the candidates to have the same transverse momentum distributions. On the right, that after weighting the $B_s^0 \to D_s^- \pi^+$ and $B_s^0 \to J/\psi\,\phi$ candidates to match the momentum distribution of $B_s^0 \to D_s^+ D_s^-$ decays the calibrations show good agreement.

	$p_0 - \langle\eta\rangle$	p_1
$B_s^0 \to D_s^- \pi^+$	0.0005 ± 0.0009	0.981 ± 0.007
$B_s^0 \to J/\psi\,\phi$	0.0000 ± 0.0005	0.975 ± 0.006
$B_s^0 \to D_s^+ D_s^-$	0.0027 ± 0.0028	1.066 ± 0.021
	After Weighting	
$B_s^0 \to D_s^- \pi^+$	-0.0010 ± 0.0009	1.031 ± 0.007
$B_s^0 \to J/\psi\,\phi$	0.0019 ± 0.0009	1.013 ± 0.007
$B_s^0 \to D_s^+ D_s^-$	0.0027 ± 0.0028	1.066 ± 0.021

Table 1: SSK calibration in different Monte Carlo samples.

sample are consistent with the expectations for a well-calibrated tagger.

$$\begin{aligned} p_0 - \langle\eta\rangle &= 0.004 \pm 0.002\,(\text{stat}), \\ p_1 &= 0.980 \pm 0.016. \end{aligned}$$

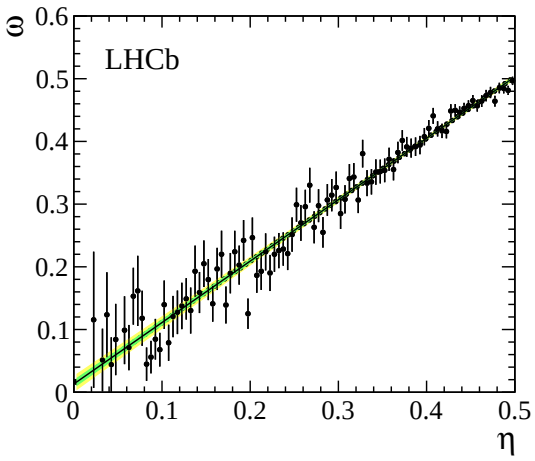

Figure 4: The data points show the averaged mistag ω in bins of η for $B^*_{s2}(5840)^0$ candidates in simulation. These candidates have been weighted to match the $B^0_s \to D^-_s \pi^+$ transverse momentum distribution. The black line corresponds to a linear fit to this distribution; the green and yellow bands are the 68% and 95% confidence level regions.